Transactions of the **14th International Conference on Structural Mechanics in Reactor Technology** (SMiRT 14), Lyon, France, August 17-22, 1997

Strength of short-radius thin-walled pipe elbows under in-plane bending loads

Nakamura K.[(1)], Wada H.[(2)], Nakamura H.[(1)], Matsuura S.I.[(1)]
(1) Central Research Institute of Electric Power Industry, Japan
(2) Mitsubishi Heavy Industries, Japan

ABSTRACT

Collapse strength of short-radius pipe elbows under in-plane bending loads has been studied based on experiments and finite element analyses. A short-radius elbow is that whose radius of curvature R of the pipe axis is nearly equal to the outer diameter Do. It was observed that for 90 degrees elbows, a short-radius elbow was stronger than a long-radius elbow where R=1.5Do, while the difference was negligible for 180 degrees elbows.

INTRODUCTION

Short-radius elbows are planned to be used in the primary sodium piping system of the demonstration FBR of Japan. A short-radius elbow is that whose radius of curvature R of the pipe axis is nearly equal to the outer diameter Do of the pipe. With short-radius elbows it is expected to make the piping design more compact and economical than with long-radius elbows for which R is about 1.5Do.

However, existing data on the strength of short-radius elbows are scarce especially in the region of large diameter thin-walled geometry where FBR piping systems are designed. In order to obtain basic data on short-radius elbows in this region, experiments have been done on three 90 degrees pipe elbows made of type 304 stainless steel with the 10-inch outer diameter. The pipe factor λ, which is defined as Rt/r^2 where r is the average radius of the pipe cross-section and t is the thickness of the pipe, ranged from 0.0608 to 0.1038.

Finite element analyses were also performed to simulate the experiments as well as to study the effect of the bend angle and the bend radius.

EXPERIMENTS

specimens

Test specimens were 10B (10-inch) 90 degrees short-radius elbows with straight pipes about five times the diameter long attached on both ends. The material of the specimens was type 304 stainless steel. The material plates were first cold-bent into the shape and welded axially at the intrados, and then solution-treated for 20 minutes at 1020°C. The geometry of the specimens are shown in Fig.1 with the configuration of the test equipment. The pipe factors of the specimens 1,2 and 3 were 0.0608, 0.0753 and 0.1038 respectively. The mechanical properties of the material were obtained with tension specimens taken from the material plate processed in the same heat treatment as the elbow specimens .

test conditions

In-plane bending displacements were applied on the specimens at room temperature. The displacement was applied first in the direction to close the elbow up to the amount about twice the displacement where the reaction force attained the maximum. Then the displacement was reversed into the opening direction and applied until the reaction force reached the equipment load limit. The load was applied for three cycles.

test results

The load-displacement relations of specimens 1,2 and 3 are shown in Fig.2. In all the cases the behavior of the specimens were quasi-static and no sudden decrease of load was observed at and after the maximum. In the opening direction of the elbow, the maximum load was not attained in any of the cases. Fig.3 shows the same results for cases 1 and 3 expressed as the relation between the rotation angle of the elbow part of the specimen and the bending moment. The maximum moment was attained when the rotation angle was about 5 degrees for both cases. The maximum loads are summarized in Table 1 with the geometry and the material data. The strength is compared to the limit load of straight pipe made of elastic perfectly-plastic material. The results are discussed later with the results of analysis.

The representative strain behaviors are shown in Fig.4 and Fig.5. Fig.4 shows the strains at the outer surface of the crown of specimen 1 plotted against the load. The circumferential strain increases with the cycle while in the axial strain the increase is not clear. Fig.5 shows these strains plotted against the rotation angle. It is observed that the relation between the strain and the rotation angle is more or less linear though the initial direction of the curve undergoes a slight change at about the rotation angle of 2 degrees, where the moment-rotation relation enters the global plasticity region (see Fig.3). A similar data was obtained in specimen 2 and shown in Fig.6.

The cross-sectional deformation was measured at the center of the elbow. The radial displacement was obtained at every 30 degrees and the data were processed with the Fourier analysis. The results are shown in Fig.7 for the specimen 2. It shows the change of the coefficient of each Fourier term with increasing displacement. It is noted that the cos (2θ) term is the most dominant and that the second important term is that of cos (4θ), which is negligible at the beginning of the load.

In some cases it may be of interest to obtain the deformation at the maximum load. Table 2 shows the results of the present tests. There is a considerable scatter but the deformation d* at the maximum load can be estimated to be at least 3 times the fictitious elastic deformation de* corresponding to the maximum load.

The instability under the deformation controlled condition depends on the compliance of the system to which the component of interest is attached. The necessary elastic follow-up factors q* for the present specimens to become unstable when the displacement d reached d** were evaluated and are shown in Table 3. The value of d** was taken as 2d* for instance. The factors are very large for all cases, indicating the deformation controlled instability to be very unlikely.

ANALYSIS

Large-displacement elastic plastic analyses were performed using the general purpose finite element analysis program MARC. Three dimensional shell elements were used. The analysis cases and the results are shown in Table 4. The first three cases are simulation of the tests. The thickness of the elbow and the material properties used in the analyses were those obtained for each specimen. The comparison to the test results of case 3 are shown in Fig.8 as an example. Though the analytical prediction under-estimates the collapse load by about 5 percent, the agreement is fair. Analysis cases 4 to 7 are to study the difference between long and short-radius elbows and between 90 degrees and 180 degrees elbows. The results are discussed below with the test results.

DISCUSSION

The test and analysis results are summarized in Fig.9 with those from literature [1], [2], [4] ~ [6]. It is observed that the collapse loads of 90 degrees short-radius elbows are generally higher than those of long-radius elbows. The average trend of experimental data in Fig.9 is expressed by $m=1.54\ \lambda^{0.779}$ for short-radius elbows, including the present data, and by $m=1.17\ \lambda^{0.768}$ for long-radius elbows, where m represents M_L/M_S. This means that, expressed relative to the corresponding straight pipe, the strength of a short radius elbow is about 1.3 times higher than a long-radius elbow with the same pipe factor. However for 180 degrees elbows there is virtually no difference between short and long-radius elbows. Therefore the difference in 90 degrees elbow is attributed to the effect of the tangent pipes. This is in accord with the agreement of 180 degrees elbow analysis cases with the prediction with the ring element analysis of Reference [1] . The lower bound of Reference [2] is actually below all the test and analysis data.

Fig.9 also shows the design standard strength indicated in Reference [3]. It is shown that 90 degrees short-radius elbows have the collapse strength at least 1.3 times that stated in the present design standard. This is in addition to the safety factors included in the allowable stress.

CONCLUSION

A 90 degrees short-radius elbow has greater collapse strength than a long-radius elbow with the same bend angle and the pipe factor. This is due to greater constraint effect by the tangent pipes.

ACKNOWLEDGMENT

This study was carried out as part of the project of the Ministry of International Trade and Industry, titled "Verification Tests of Fast Breeder Reactor Technology", which has been conducted since 1987. Authors gratefully acknowledge the helpful discussions by Prof. H. Akiyama, Prof. H. Ohtsubo (University of Tokyo) and Prof. Yamada (Tohoku University) throughout the course of this work.

REFERENCES

1. Wtanabe,O. and H.Ohtsubo 1976. Elastic-plastic analysis of pipe bends subjected to in-plane bending. Theoretical and Applied Mechanics, volume26, *Proc. 26th Japan National Congress for Applied Mechanics.*

2. Spence,J. and G.E.Findlay 1973. Limit loads for pipe bends under in-plane bending.*2nd International Conference on Pressure Vessel and Piping,* I-28.

3. ASME Boiler and Pressure Vessel Code Section III, NB3600,1995.

4. Gross,N. 1952-53. Experiments on short-radius pipe-bends. *Proc. Inst. Mech. Engrs. 1B,* pp331-345.

5. Bolt,S.E. and W.L.Greenstreet 1971. Experimental determinations of plastic collapse loads for pipe elbows. *ASME publication* 71-PVP-37.

6. Imazu,A., Y.Sakakibara, T.Nagata, and T.Hashimoto 1981. Plastic instability test of elbows under in-plane and out-of-plane bending. Trans. 6th SMiRT E6/5.

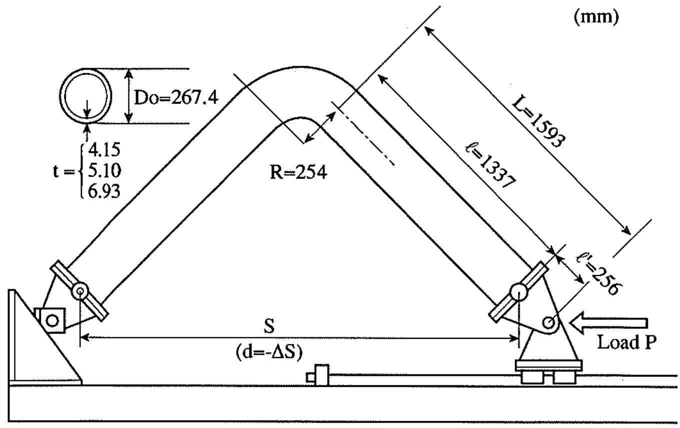

Fig.1 Specimen and Equipment

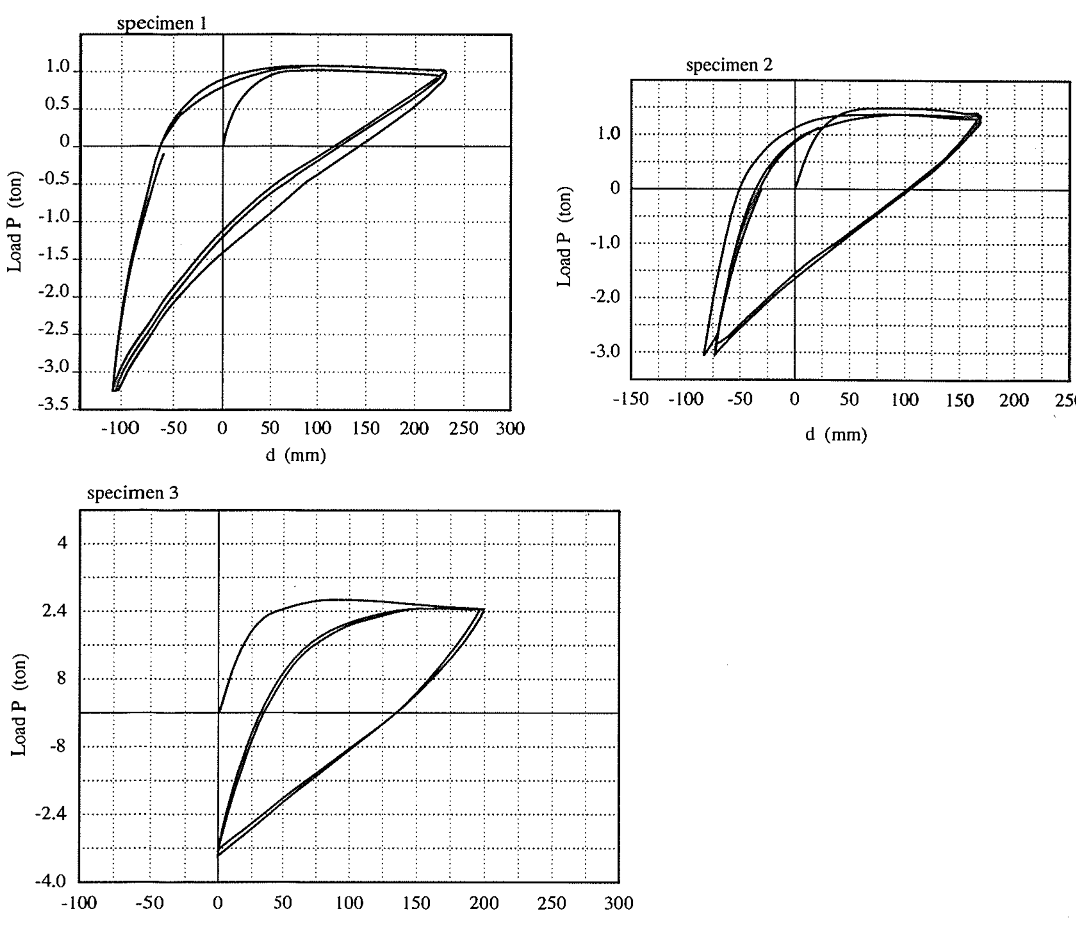

Fig.2 Load-Displacement Relations

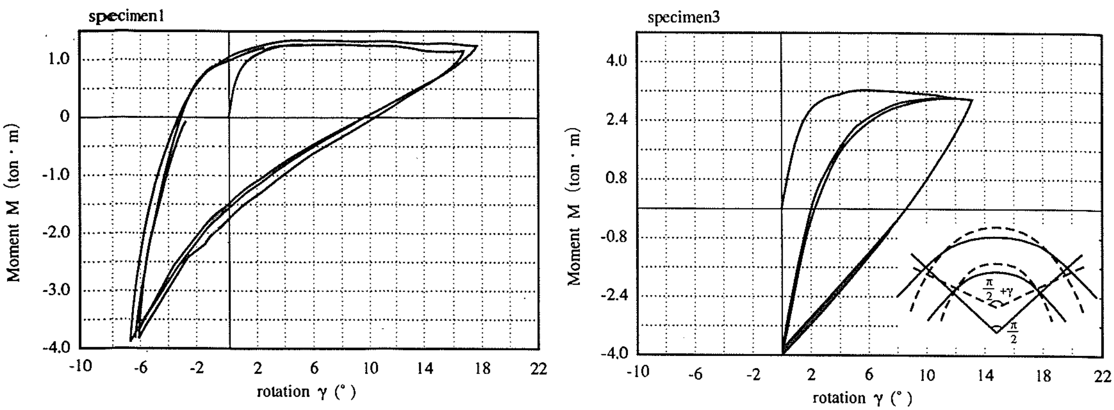

Fig.3 Moment-Rotation Relations

Table1 Specimen Details and Test Results

SUS304, RT

specimen			1 (10B Sch5S)	2 (10B Sch10S)	3 (10B Sch20S)
outer diameter	Do	(mm)	267.4	267.4	267.4
wall thickness	t (measured average)	(mm)	4.15	5.10	6.93
bend radius	R	(mm)	254.0	254.0	254
average radius	r=(Do-t)/2	(mm)	131.625	131.15	130.235
pipe factor	$\lambda=Rt/r^2$		0.0608	0.0753	0.1038
material yield stress	σ_y (measured average)	(kgf/mm^2)	24.72	26.44	24.58
maximum load	Pmax	(kgf)	1070	1460	2660
maximum bending moment	ML=Pmax•a (a=1200.8mm)	(kgf · mm)	1.285×10^8	1.753×10^8	3.194×10^8
ML/Z	($Z=\pi r^2 t$)	(kgf/mm^2)	5.688	6.362	8.650
collapse moment of straight pipe	$M_S=4r^2t\sigma_y$	(kgf · mm)	7.109×10^8	9.277×10^8	1.156×10^7
Ms/Z		(kgf/mm^2)	31.47	33.66	31.30
ML/Ms			0.1807	0.1890	0.2764

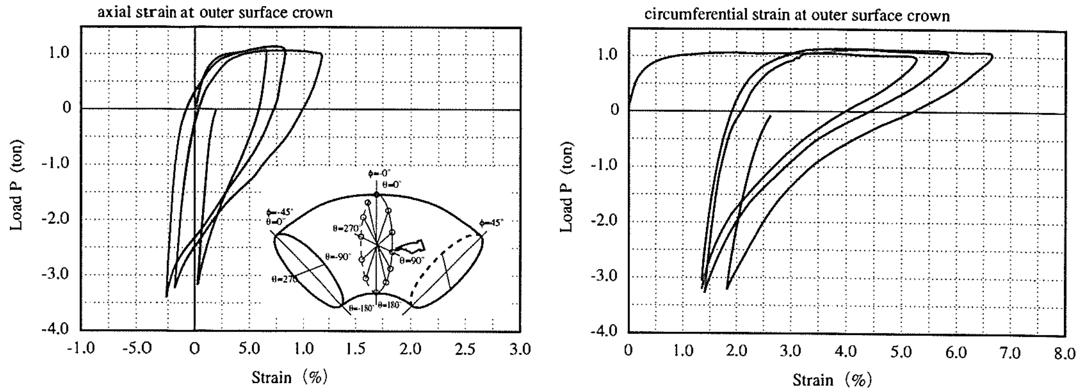

Fig.4 Strain behavior of specimen 1

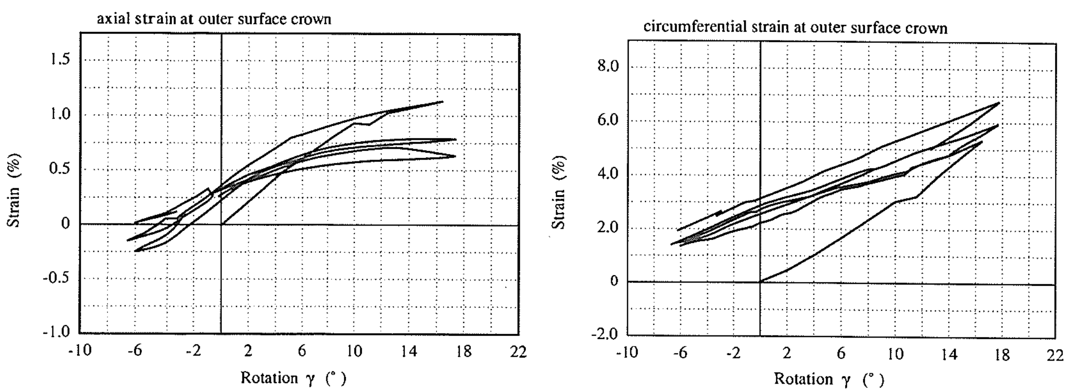

Fig.5 Strain vs rotation (specimen 1)

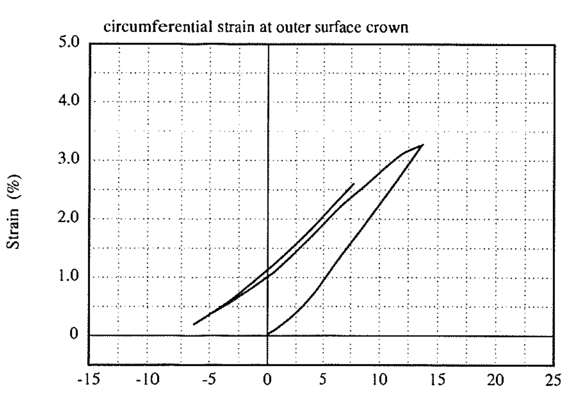

Fig.6 Strain vs rotation (specimen 2)

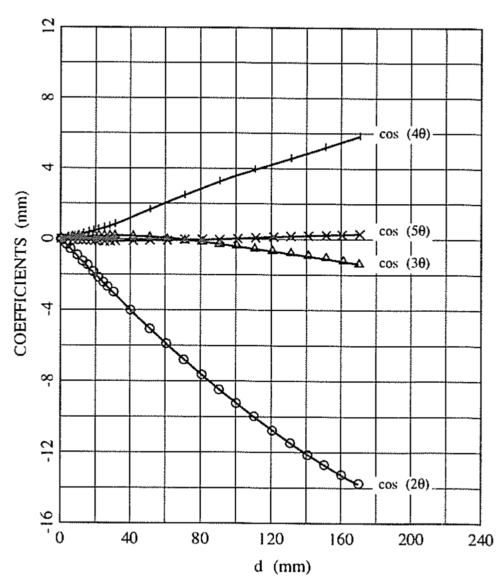

Fig.7 Cross-section deformation Fourier analysis (specimen 2)

Table2 Displacement at Maximum Load

specimen	1 (10B Sch5S λ=0.0608)	2 (10B Sch10S λ=0.0753)	3 (10B Sch20S λ=0.1038)
displacement d* at max. load P_{max} (mm)	114	85	100
elastic spring constant $k=(P/d)_{elastic}$ (kgf/mm)	47.5	65.5	121
$de^*=P_{max}/k$ (mm)	22.5	22.3	22.0
d*/de*	5.07	3.81	4.55

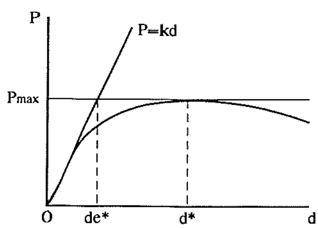

Table3 Conditions for Instability at d=d** (d** taken as 2d*)

specimen	1 (10B Sch5S λ=0.0608)	2 (10B Sch10S λ=0.0753)	3 (10B Sch20S λ=0.1038)
d** (mm)	228	170	200
P** (kgf)	980	1360	2460
Pe (kgf)	1160	1590	2980
k (kgf/mm)	47.5	65.5	121
de=Pe/k (mm)	24.4	24.3	24.6
q*	54.7	42.5	41.8

(note) $\frac{Pe - P^{**}}{k} / (d^{**} - de) = 1/(q^* - 1)$

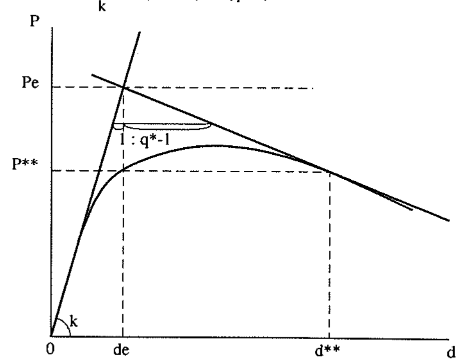

Table4 Analysis Conditions and Results

[unit : kgf, mm]

Case	1	2	3	4	5	6	7
	90°elbow					180°elbow	
Short or Long	Short	Short	Short	Long	Long	Short	Long
Do	267.4	267.4	267.4	267.4	267.4	267.4	267.4
R	254	254	254	381	381	254	381
t	4.15	5.10	6.93	3.4	5.10	5.10	3.4
r=(Do-t)/2	131.625	131.15	130.235	131.15	131.15	131.15	131.15
$\lambda=Rt/r^2$	0.0608	0.0753	0.1038	0.0753	0.1130	0.0753	0.0753
ts (thickness of tangent pipes)	3.97	3.88	6.20	2.587	3.88	3.88	2.587
E	20400	20620	21030	20620	20620	20620	20620
ν	0.286	0.286	0.268	0.286	0.286	0.286	0.286
σy (0.2% proof stress)	24.72	26.44	24.58	26.44	26.44	26.44	26.44
Elbow strength M_L/Z ($Z=\pi r^2 t$)	5.40	6.13	8.227	5.074	7.359	5.07	5.33
Straight pipe strength M_S/Z ($=\frac{4}{\pi}\sigma y$)	31.47	33.66	31.30	33.66	33.66	33.66	33.66
M_L/M_S	0.176	0.182	0.236	0.151	0.2186	0.1507	0.1585

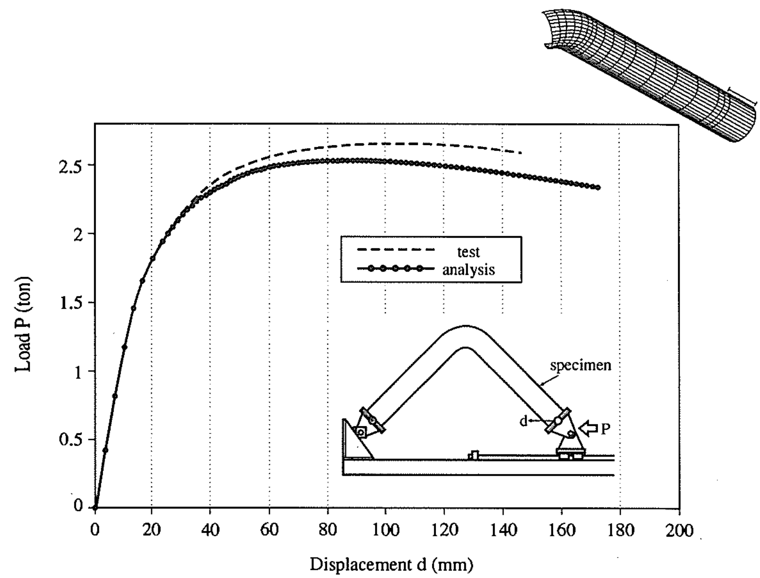

Fig.8 Comparison between test and analysis results (specimen 3)

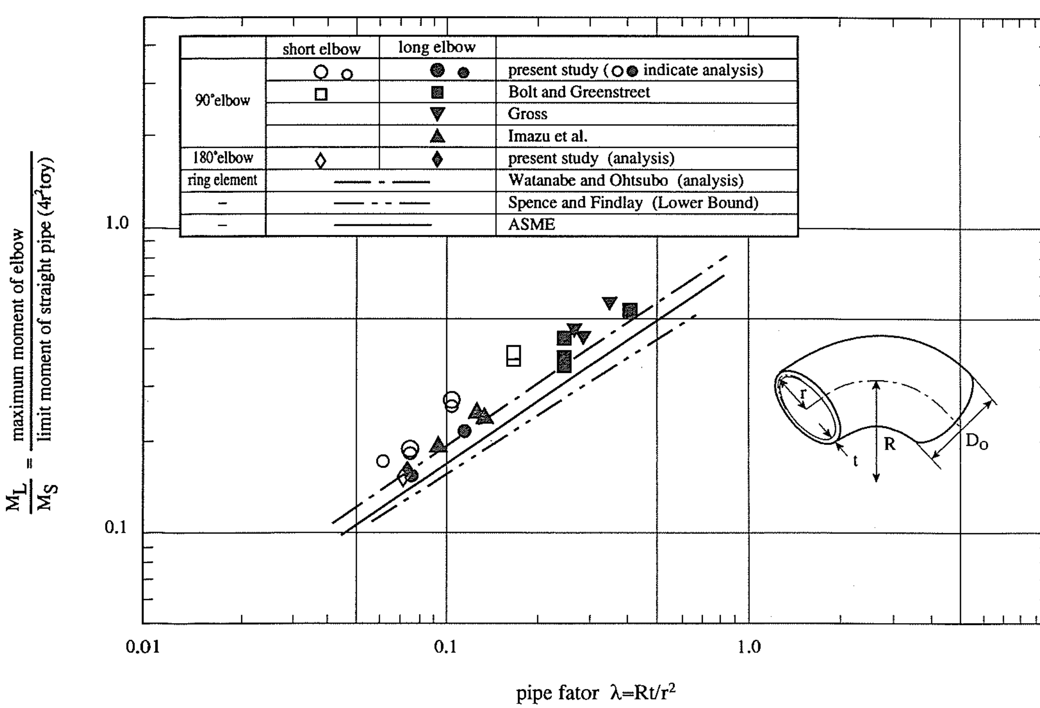

Fig.9 Strength of elbows subjected to in-plane bending